ACTA MECHANICA SINICA (English Series), Vol.13, No.3, August 1997 ISSN 0567-7718
The Chinese Society of Theoretical and Applied Mechanics
Chinese Journal of Mechanics Press, Beijing, China
Allerton Press, INC., New York, U.S.A.

NUMERICAL MODELING OF 3-D TURBULENT TWO-PHASE FLOW AND COAL COMBUSTION IN A PULVERIZED-COAL COMBUSTOR*

Zhou Biao** (周 彪) Wu Chengkang (吴承康)
(*Combustion Laboratory, Institute of Mechanics, Chinese Academy of Sciences, Beijing* 100080, *China*)

ABSTRACT: In the present paper, a multifluid model of two-phase flows with pulverized-coal combustion, based on a continuum-trajectory model with reacting particle phase, is developed and employed to simulate the 3-D turbulent two-phase flows and combustion in a new type of pulverized-coal combustor with one primary-air jet placed along the wall of the combustor. The results show that: (1) this continuum-trajectory model with reacting particle phase can be used in practical engineering to qualitatively predict the flame stability, concentrations of gas species, possibilities of slag formation and soot deposition, etc.; (2) large recirculation zones can be created in the combustor, which is favorable to the ignition and flame stabilization.

KEY WORDS: numerical simulation, pulverized-coal combustor, two-phase flow

1 INTRODUCTION

It is well known that the particle trajectory model[1,2] has been most widely used in modeling pulverized-coal combustion. With this model, the particle history effect can be easily taken into account and false diffusion can be avoided in modeling particle phase, but it is difficult for this model to fully consider the turbulent transport of particle mass, particle momentum and particle energy, and is difficult to give detailed information of particle velocity and concentration comparable with experimental results. In order to compare the predictions with the experimental results, it is necessary to calculate a large number of trajectories. At the same time, the pure trajectory model suffers from the difficulty in dealing with particle entering or leaving the recirculating zone. The continuum model can fully account for the particle turbulent transport, and can give more detailed information which can be compared with experimental results, but it is difficult to consider the particle history effect. The continuum-trajectory model with reacting particle phase, proposed by Prof. L. X. Zhou[3,4], overcomes these disadvantages and retains the advantages of both models mentioned above. This model has been successfully used in modeling 2-D pulverized-coal combustion[5].

Received 6 January 1997
* Sponsored by the National Key Projects of Fundamental Research of China.
** Present Address: Department of Mechanical and Aerospace Engineering, Princeton University, Princeton, NJ 08544, USA

A new type of pulverized-coal combustor possibly having multiple functions and low pollutant emission has been proposed[6]. The chief aims are to increase the residence time of coal particles and to solve the problem of slag formation in the combustor. Figure 1 shows the schematic diagram of the combustor. A pair of primary air jets and a pair of control jets enter the combustor along the wall, as shown in the figure. The air jets along the wall can effectively protect it against overheating and erosion and can effectively solve the problem of slag formation. The flowfield characteristics may be utilized to achieve a multiple of functions, which include boiler startup, low load flame stabilization and main burner operation. As the first step of research, 3-D numerical simulation of two-phase flow in this combustor has been carried out. Some useful guidelines have been obtained through this work.

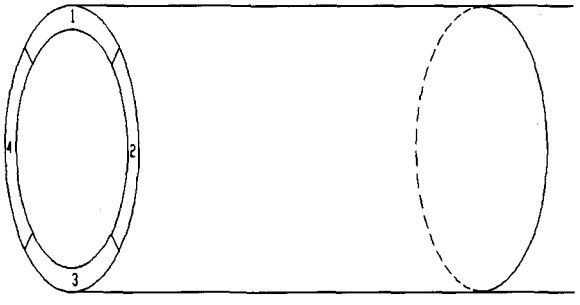

Fig.1 Schematic diagram of the proposed combustor
1,3—primary air; 2,4—controlling air

In the present paper, in order to develop the computer code of this multifluid model of two-phase flows with pulverized-coal combustion, the calculation conditions are simplified. In the simplified case, the controlling jets (air jets No.2 and 4) and one primary-air jet (air jet No.3) are turned off and the remaining primary-air (air jet No.1) is turn on. A 180° sector is taken as the computed domain in the r-θ plane. The primary-air inlet is located in the x-r plane of $\theta = 0°$. Some important results are obtained.

2 NUMERICAL MODELS AND SOLUTION PROCEDURE

Based on the continuum concept of multiphase flows and the k-ε-Ap two-phase turbulence model[7], the gas phase governing equations for 3-D turbulent reacting gas-particle flows in cylindrical coordinates can be written in the following generalized form

$$\frac{\partial}{\partial x}(\rho u\phi) + \frac{1}{r}\frac{\partial}{\partial r}(r\rho v\phi) + \frac{1}{r}\frac{\partial}{\partial \theta}(\rho w\phi) = \frac{\partial}{\partial x}(\Gamma_\phi \frac{\partial \phi}{\partial x}) + \frac{1}{r}\frac{\partial}{\partial r}(r\Gamma_\phi \frac{\partial \phi}{\partial r}) + \frac{1}{r^2}\frac{\partial}{\partial \theta}(\Gamma_\phi \frac{\partial \phi}{\partial \theta}) + S_\phi + S_{\phi p} \qquad (\phi = 1, u, v, w, k, \varepsilon, h, Y_s) \qquad (1)$$

The meanings of ϕ, Γ_ϕ and S_ϕ are the same as those in modeling of pure gas phase, and $S_{\phi p}$ is $-\sum n_k \dot{m}_k$, $-\sum \frac{\rho_k}{\tau_{rk}}(u-u_k) - u\sum n_k \dot{m}_k$, $-\sum \frac{\rho_k}{\tau_{rk}}(v-v_k) - v\sum n_k \dot{m}_k$, $-\sum \frac{\rho_k}{\tau_{rk}}(w-w_k) - w\sum n_k \dot{m}_k$, 0 , 0 , $\sum n_k \dot{m}_{sk}$, $\sum n_k Q_k - h\sum n_k \dot{m}_k$, $-\alpha_s \sum n_k \dot{m}_k$, in different equations, and the subscript s denotes CH_4, CO, CO_2, O_2 and H_2O.

The time-averaged reaction rate is determined by the EBU-Arrhenius model:

$$W_s = \min(W_{s\cdot\mathrm{EBU}}, W_{s\cdot\mathrm{Ar}})$$

$$W_{s\cdot\mathrm{EBU}} = C_R \rho Y_{\mathrm{FU}}^2 \varepsilon / k$$

$$W_{s\cdot\mathrm{Ar}} = B_s \rho^2 Y_s Y_{\mathrm{OX}} \exp(-E/RT) \qquad (s = \mathrm{CH_4}, \mathrm{CO})$$

where W is reaction rate, Y is mass fraction, subscript Ar denotes Arrhenius Law, EBU denotes eddy-break-up model, FU denotes fuel.

The time-averaged particle-phase continuity and momentum equations for 3-D turbulent reacting gas-particle flows in cylindrical coordinates can be written in the following generalized form

$$\frac{\partial}{\partial x}(\rho_k u_k \phi_k) + \frac{\partial}{r\partial r}(r\rho_k v_k \phi_k) + \frac{\partial}{r\partial\theta}(\rho_k w_k \phi_k) = \frac{\partial}{\partial x}(\Gamma_\phi \frac{\partial \phi_k}{\partial x}) + \frac{\partial}{r\partial r}(r\Gamma_\phi \frac{\partial \phi_k}{\partial r}) + \frac{\partial}{r^2\partial\theta}(\Gamma_\phi \frac{\partial \phi_k}{\partial \theta}) + S_{\phi k} + S_{\phi kg} \tag{2}$$

where ϕ_k, Γ_ϕ, $S_{\phi k}$ and $S_{\phi kg}$ denote the generalized variable, transport coefficient and source term of particle phase respectively, and their meanings for each equation are shown in Tab.1.

The equations of mass and temperature change of a pulverized-coal particle, using the two-equation model of devolatilization and three-reaction model of diffusion-kinetic char combustion, can be written as follows[7]

$$\dot{m}_k = \dot{m}_{kw} + \dot{m}_{kv} + \dot{m}_{hk}$$

$$\dot{m}_{kw} = \pi d_k Nu D \rho \ln[1 + (Y_{ww} - Y_{w\infty})/(1 - Y_{ww})]$$

$$Y_{ww} = B_w \exp(-E_w/RT_k)$$

$$\dot{m}_{kv} = m_{ck} \alpha B_v \exp(-E_v/RT_k)$$

$$\frac{\mathrm{d}m_{ck}}{\mathrm{d}t} = -m_{ck} B_v \exp(-E_v/RT_k)$$

$$\dot{m}_{hk} = \sum[\pi d_k Y_{sw} \sum B_1 \exp(-E_1/RT_k)]$$

$$\frac{\pi d_k^3}{6}\rho_p C_c \frac{\mathrm{d}T_k}{\mathrm{d}t} = \pi d_k^2 \sigma \varepsilon (T^4 - T_k^4) - \dot{m}_k q_w + \dot{m}_{hk} Q_c$$

where subscript w denotes wall, g denotes gas, v denotes volatile, c denotes raw coal, and p denotes particle.

The particle mass and temperature change due to reactions is traced along the trajectories obtained from the Eulerian predictions, by using these ordinary differential equations and algebraic expressions. These ordinary differential equations are solved by using 4th order Runge-Kutta method [8].

The particle turbulence is modeled by using the particle-tracking-fluid (Ap) model

$$\frac{\nu_k}{\nu_T} = (1 + \frac{\tau_{rk}}{\tau_T})^{-1}$$

where

$$\tau'_{rk} = \frac{d_k^2 \rho_p}{18\mu} \qquad \tau_T = 1.5 C_\mu k/\varepsilon$$

Table 1 Equations for particle phase

Equations	ϕ_k	α	β	$\Gamma_{\phi k}$	$S_{\phi k}$	$S_{\phi kg}$
Particle continuity	1	ρ_k	ρ_k	$\frac{\nu_k}{\sigma_p}$	$n_k\dot{m}_k$	0
Particle axial momentum	u_k	ρ_k	1	μ_k	$\frac{\partial}{\partial x}(\mu_k\frac{\partial u_k}{\partial x})+\frac{\partial}{r\partial r}(r\mu_k\frac{\partial v_k}{\partial x})+$ $\frac{\partial}{r\partial\theta}(\mu_k\frac{\partial w_k}{\partial x})+\frac{\partial}{\partial x}(u_k\frac{\nu_k}{\sigma_p}\frac{\partial\rho_k}{\partial x})+$ $\frac{\partial}{r\partial r}(ru_k\frac{\nu_k}{\sigma_p}\frac{\partial\rho_k}{\partial r})+\rho_k g_x+$ $\frac{\partial}{r^2\partial\theta}(\mu_k\frac{\nu_k}{\sigma_p}\frac{\partial\rho_k}{\partial\theta})+\frac{\partial}{\partial x}(u_k\frac{\nu_k}{\sigma_p}\frac{\partial\rho_k}{\partial x})+$ $\frac{\partial}{r\partial r}(rv_k\frac{\nu_k}{\sigma_p}\frac{\partial\rho_k}{\partial x})+\frac{\partial}{r\partial\theta}(w_k\frac{\nu_k}{\sigma_p}\frac{\partial\rho_k}{\partial x})$	$\frac{\rho_k}{\tau_{rk}}(u-u_k)+$ $un_k\dot{m}_k$
Particle radial momentum	v_k	ρ_k	1	μ_k	$\frac{\partial}{\partial x}(\mu_k\frac{\partial u_k}{\partial r})+\frac{\partial}{r\partial r}(r\mu_k\frac{\partial v_k}{\partial r})+\frac{1}{r}\rho_k w_k^2+$ $\frac{\partial}{r\partial\theta}[\mu_k(\frac{\partial w_k}{\partial r}-\frac{w_k}{r})]-\frac{2}{r}\mu_k(\frac{\partial w_k}{r\partial\theta}+\frac{v_k}{r})+$ $\frac{\partial}{\partial x}(v_k\frac{\nu_k}{\sigma_p}\frac{\partial\rho_k}{\partial x})+\frac{\partial}{r\partial r}(rv_k\frac{\nu_k}{\sigma_p}\frac{\partial\rho_k}{\partial r})+$ $\frac{\partial}{r^2\partial\theta}(v_k\frac{\nu_k}{\sigma_p}\frac{\partial\rho_k}{\partial\theta})+\frac{\partial}{\partial x}(u_k\frac{\nu_k}{\sigma_p}\frac{\partial\rho_k}{\partial r})+$ $\frac{\partial}{r\partial r}(rv_k\frac{\nu_k}{\sigma_p}\frac{\partial\rho_k}{\partial r})+\frac{\partial}{r\partial\theta}(w_k\frac{\nu_k}{\sigma_p}\frac{\partial\rho_k}{\partial r})-$ $\frac{2}{r^2}w_k\frac{\nu_k}{\sigma_p}\frac{\partial\rho_k}{\partial\theta}+\rho_k g_r$	$\frac{\rho_k}{\tau_{rk}}(v-v_k)+$ $vn_k\dot{m}_k$
Particle tangential momentum	w_k	ρ_k	1	μ_k	$\frac{\partial}{\partial x}(\mu_k\frac{\partial u_k}{r\partial\theta})+\frac{\partial}{r\partial r}[r\mu_k(\frac{\partial v_k}{r\partial\theta}-\frac{w_k}{r})]+$ $\rho_k g_\theta+\frac{\partial}{r\partial\theta}[\frac{\mu_k}{r}(\frac{\partial w_k}{\partial\theta}+2v_k)]-$ $\frac{1}{r}\rho_k v_k w_k+\frac{\mu_k}{r}(\frac{\partial v_k}{r\partial\theta}+\frac{\partial w_k}{\partial r}-\frac{w_k}{r})+$ $\frac{\partial}{\partial x}(w_k\frac{\nu_k}{\sigma_p}\frac{\partial\rho_k}{\partial x})+\frac{\partial}{r\partial r}(rw_k\frac{v_k}{\sigma_p}\frac{\partial\rho_k}{\partial r})+$ $\frac{\partial}{r^2\partial\theta}(w_k\frac{\nu_k}{\sigma_p}\frac{\partial\rho_k}{\partial\theta})+\frac{\partial}{\partial x}(u_k\frac{\nu_k}{\sigma_p}\frac{\partial\rho_k}{r\partial\theta})+$ $\frac{\partial}{r\partial r}(rv_k\frac{\nu_k}{\sigma_p}\frac{\partial\rho_k}{r\partial\theta})+\frac{\partial}{r\partial\theta}(w_k\frac{\nu_k}{\sigma_p}\frac{\partial\rho_k}{r\partial\theta})+$ $\frac{w_k}{r}\frac{\nu_k}{\sigma_p}\frac{\partial\rho_k}{\partial r}+\frac{v_k}{r^2}\frac{\nu_k}{\sigma_p}\frac{\partial\rho_k}{\partial\theta}$	$\frac{\rho_k}{\tau_{rk}}(w-w_k)+$ $wn_k\dot{m}_k$

Both gas-phase and particle-phase conservation equations in the Eulerian coordinates are integrated in the computational cell to obtain the finite difference equations by using the hybrid scheme for the convection terms, and the linearization of the source terms. The finite difference equations are solved by TDMA line-by-line and plane-by-plane iterations with under-relaxation[9]. Multiple iterations between the two phases have been adopted.

Some additional formulas are shown in Table 2. The grid system contains $33\times18\times14=8316$ nodes in the computational domain (ϕ300 mm $\times$1200mm). The initial diameter of coal particles is 60 μm. The computer code has been developed with nearly 20000 FORTRAN77

Table 2 Additional formulas

$G_k = \mu_T\Big\{2\big[(\frac{\partial u}{\partial x})^2+(\frac{\partial v}{\partial r})^2+(\frac{1}{r}\frac{\partial w}{\partial \theta}+\frac{v}{r})^2\big]+ (\frac{\partial w}{\partial x}+\frac{\partial u}{r\partial\theta})^2+(\frac{\partial u}{\partial r}+\frac{\partial v}{\partial x})^2+(\frac{\partial v}{r\partial\theta}+\frac{\partial w}{\partial r}-\frac{w}{r})^2\Big\}$
$\mu_e=\mu_T+\mu \quad \mu_T=C_\mu\rho k^2/\varepsilon \quad \nu_T=\mu_T/\rho$
$\mu_k=\rho_k\nu_k \quad \nu_k/\nu_T=(1+\frac{\tau'_{rk}}{\tau_T})^{-1} \quad \tau'_{rk}=\rho d_k^2/18\mu$
$\tau_T=C_T k/\varepsilon \quad \tau_{rk}=\frac{\rho_p d_k^2}{18\mu}(1+0.15Re_k^{0.667})^{-1}\frac{\exp(B_k)-1}{B_k}$

statements, and running one case in a microcomputer 486-66 spends about 170 CPU hours.

3 RESULTS AND DISCUSSIONS

3.1 Stability of Pulverized-coal Flame

(1) Configuration of recirculation zones

Figure 2 shows that there are obvious gas and particle recirculation zones, both in $\theta = 0°, 180°$ plane and $\theta = 90°, 270°$ plane.

(2) Figure 3 is the gas-phase temperature contour map in coal combustion. It can be seen that the high temperature zones of gas phase are located in the gas and particle recirculation zones.

(3) Figure 4 gives the coal particle concentration contours in coal combustion. It can be seen that the particle concentration in the recirculation zones (especially in x-r plane of $\theta = 90°, 270°$) is high.

In summary, Fig.2 through Fig.4 illustrate that, in the combustor, there are several strongly recirculating zones, in which the particle concentration and the gas-phase temperature are high. Such features can be used to stabilize the coal flame.

3.2 Prediction of Slag Formation and Soot Deposition

The reasons of slag formation mainly include the following items: melting of coal particles due to their high temperature; high temperature of the wall of the combustor; impingement against the wall by the coal particles. The reason of soot deposition is mainly that, in the combustor, there exist dead zones in which the velocity of gas/particle is nearly zero. The melting point of the coal used in this research is about 1 573 K. From Fig.3, it can be seen that there are possibilities of slag formation and soot deposit in the combustor with only one-primary-air jet. From the velocity vectors in the r-θ planes (Fig.5), such places can be predicted. In the places where the particles impinge against the wall directly, slag may be formed; in the places where the particle/gas velocity is nearly zero, soot may be deposited.

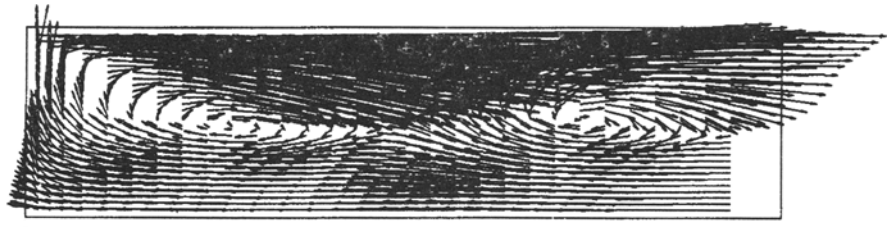

(a) gas (θ=0°, 180°)

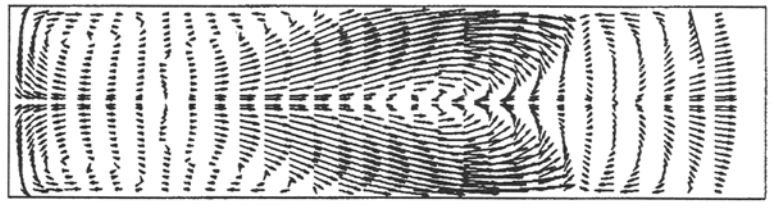

(b) gas (θ=90°, 270°)

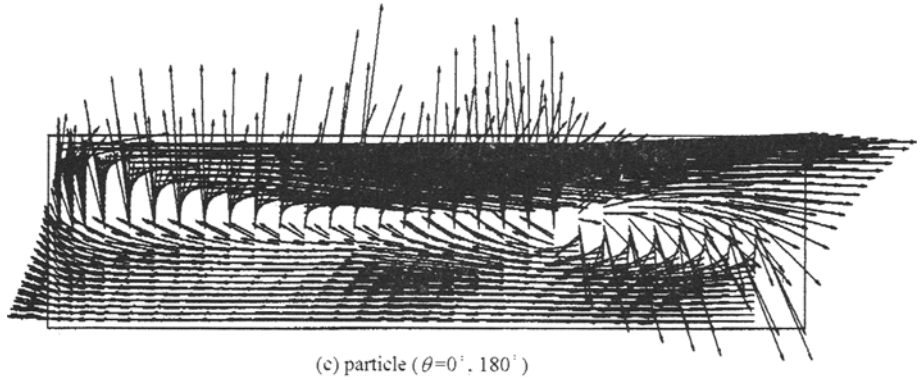

(c) particle (θ=0°, 180°)

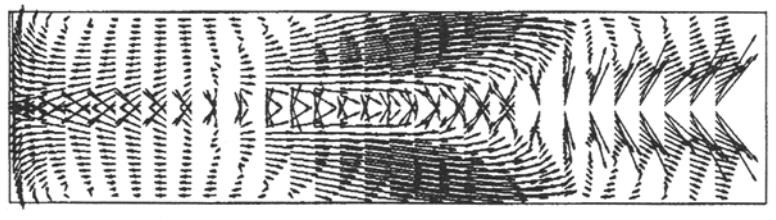

(d) particle (θ=90°, 270°)

Fig.2 Velocity vectors

3.3 Prediction of Concentration for Gas Species

Figure 6 and Fig.7(a) are the concentration contour maps for volatile and oxygen respectively. The volatile concentration in the reverse-flow zones is nearly zero except the reverse-flow zone near the outlet at the x-r plane of $\theta = 90°, 270°$ where the volatile concentration is higher due to the reverse flow of the gases at the plane of $\theta = 0°$ which contain higher concentration of unburnt volatile. The oxygen concentration in the reverse-flow zone is lower than that in other zones. Such features illustrate that these recirculation zones are very important to devolatilization, ignition, and stable combustion.

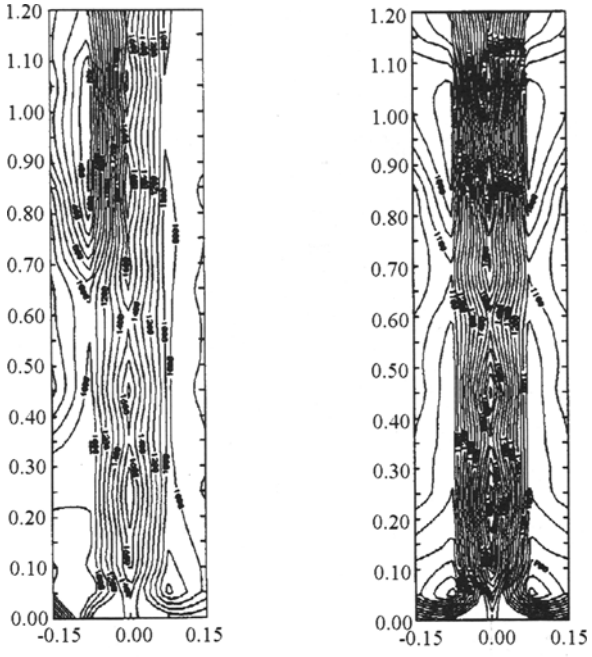

(a) θ=0°, 180° (b) θ=90°, 270°

Fig.3 Temperature contours

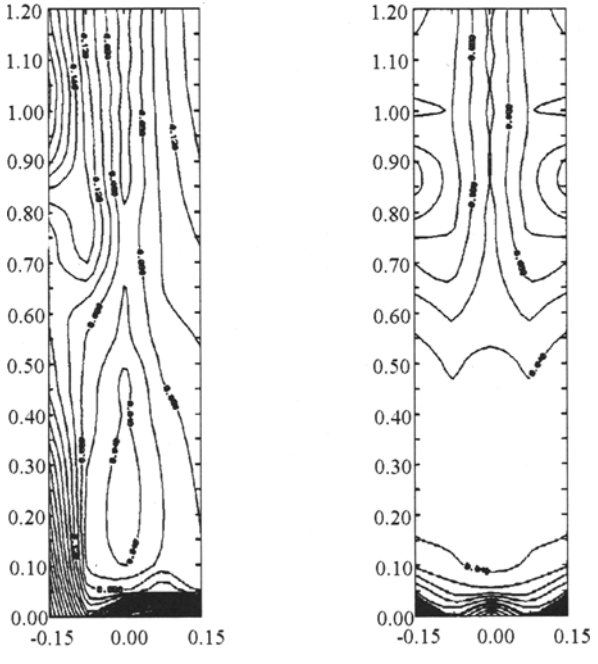

(a) θ=0°, 180° (b) θ=90°, 270°

Fig.4 Particle concentration contours

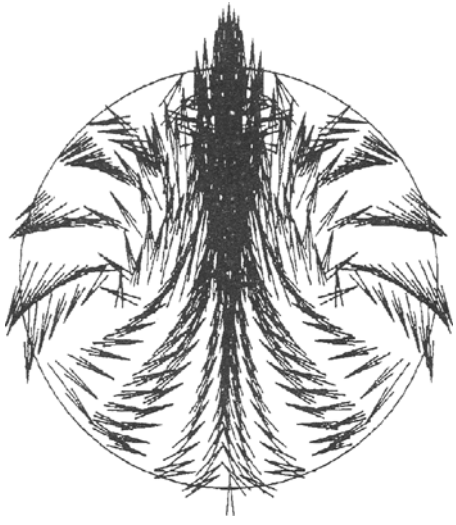

Fig.5 Velocity vectors in the r-θ planes of two-phase combustion (x=690 mm)

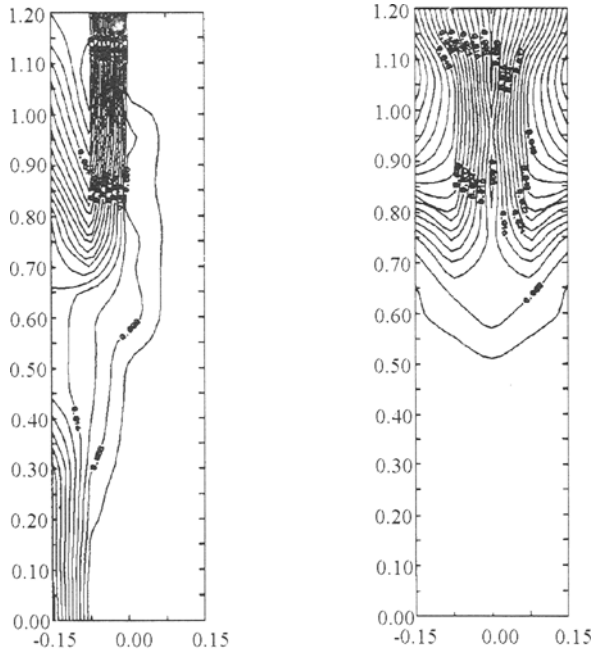

Fig.6 CH_4 concentration contours

Figure 7(b) and Fig.7(c) are the contour maps for the concentration of carbon dioxide and water vapour respectively. These concentrations in the recirculation zones are higher, which illustrates the high-temperature gases can be entrained by the recirculating flow. Such feature is beneficial to the stability of coal flame.

Figure 8 is the contour map for carbon monoxide concentration in the combustor. In the zone with axial distance x less than 0.8 m, the carbon monoxide concentration is nearly

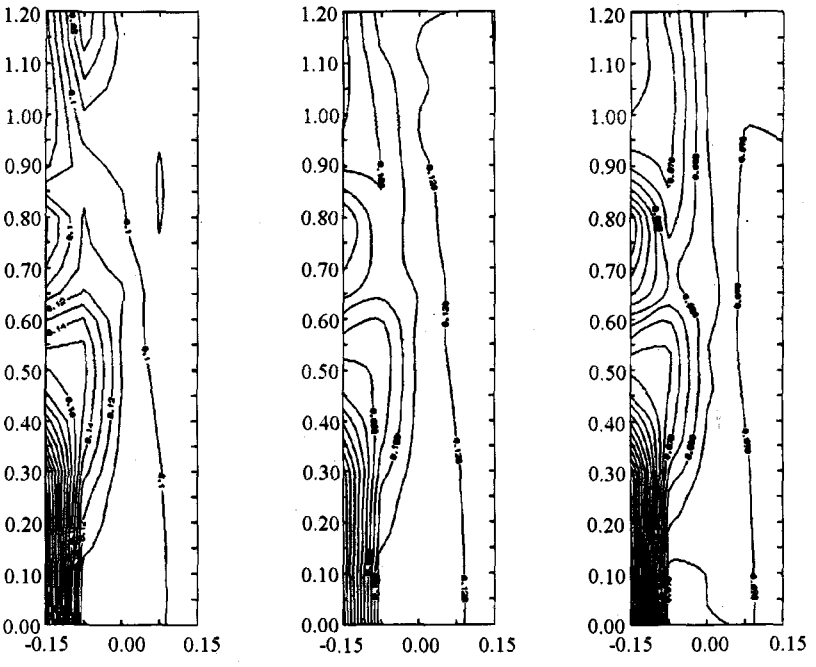

(a)O_2 (θ=0°, 180°) (b)CO_2 (θ=0°, 180°) (c)H_2O (θ=0°, 180°)

Fig.7 Concentration contours

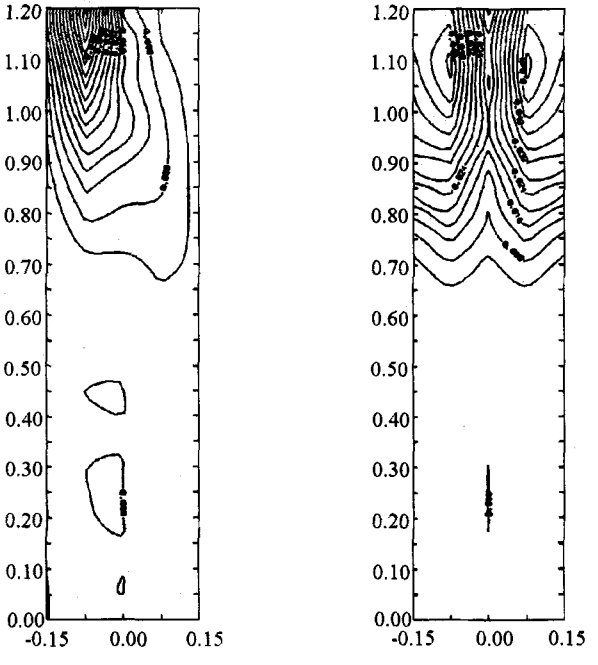

(a) two-phase combustion (θ=0°, 180°)

(b) two-phase combustion (θ=90°, 270°)

Fig.8 CO concentration contours

zero, while in other zones the carbon monoxide concentration is higher. This exactly illustrates the recirculation zone near the outlet is very important to char combustion.

4 CONCLUSIONS

(1) The computer code for the numerical modeling of 3-D turbulent two-phase flows and pulverized-coal combustion based on a continuum-trajectory model with reacting particle phase has been successfully developed and has been successfully applied to the modeling of a combustor with one primary-air inlet along its wall.

(2) The prediction can qualitatively give very useful information in practical engineering, such as, the stability of flame, possibilities of slag formation and soot deposit, concentrations of gas species, etc.; So this prediction method as an optimizing tool can be used to model the practical two-phase flows with pulverized-coal combustion in combustors or furnaces.

(3) The prediction results show that the gas and particle recirculation zones are very important to devolatilization, volatile ignition and flame stabilization, especially, the recirculation zone near the outlet at the x-r plane of $\theta = 90°$, and $270°$ is crucially important to char combustion.

Acknowledgement This work has been supported by the National Key Projects of Fundamental Research of China. We acknowledge the contribution of many other members, Professors Lifang Chen, Huanqing Zhan, and Wenchao Sun, of the Combustion Laboratory, Institute of Mechanics, Chinese Academy of Sciences.

REFERENCES

1 Smoot LD, Smith PJ. Coal Combustion and Gasification. New York: Plenum Publishing Co., 1985

2 Lockwood FC, Mahmud T. The prediction of swirl burner pulverized coal flames. Twenty-second Symposium (International) on Combustion. The Combustion Institute, Pittsburgh, PA, 1988. 165~173

3 Zhou LX, Zhang J. A Langrangian-Eulerian particle model for turbulent two-phase flows with reacting particle. In: Zhuang Fenggan ed. Proc 10th Inter Conf on Num Meth in Fluid Dyn. Berlin: Springer-Verlag, 1986. 705~709

4 Zhou LX. A multi-fluid model of two-phase flows with pulverized-coal combustion. In: Feng Junkai ed. Coal Combustion. N.Y.: Hemisphere, 1988. 207~213

5 Deng Zuobo, Zhou Lixing. Numerical modeling of the combustion of pulverized-coal in a controlled mixing-history furnace. Proc of 2nd Inter Symp on Coal Comb. Beijing: China Machine Press, 1991. 114~121

6 Zhou B, Wu Chengkang. 3-D numerical simulation of two-phase flows in a proposed pulverized-coal combustor with multiple functions and low emission of pollutants. In: Leung TP ed. Proc 3rd Asian-Pacific International Symposium on Combustion and Energy Utilization, Dec.11~15,1995, Hong Kong, Hong Kong Polytechnic University, 216

7 Zhou Lixing. Theory and Numerical Modeling of Turbulent Gas-Particle Flows and Combustion. Beijing: Science Press and Florida: CRC Press, 1993

8 Donald Greenspan, Vincenzo Casulli. Numerical Analysis for Applied Mathematics, Science, and Engineering, Addison-Wesley Publishing Company, Inc, 1988. 112~117

9 Patanker SV. Numerical Heat Transfer and Fluid Flow. Hemisphere, 1980